

# Exoplanets from the CHEPS\*: Discovery of the Double Planet System HD191760†

J.S. Jenkins<sup>1</sup>, H.R.A. Jones<sup>2</sup>, J.R. Barnes<sup>2</sup>, M.I. Jones<sup>1</sup>, P. Rojo<sup>1</sup>,

S. Hoyer<sup>1</sup>, A.C. Day-Jones<sup>2</sup>

<sup>1</sup>*Department of Astronomy, Universidad de Chile, Cerro Calan, Las Condes, Santiago, Chile, Casilla 36-D, email: jjenkins@das.uchile.cl*

<sup>2</sup>*Center for Astrophysics, University of Hertfordshire, College Lane Campus, Hatfield, Hertfordshire, UK, AL10 9AB*

Draft: 11/08

## ABSTRACT

We report the discovery of planetary companions around HD191760 with orbital periods of  $8.64 \pm 0.02$  and  $86.83 \pm 0.50$  days, semimajor axes of 0.09 and 0.42 AU and masses of  $0.29 \pm 0.05$  and  $7.20 \pm 0.44 M_J$  respectively. The star has a spectral type of G3IV/V and a metallicity of 0.29 dex. HD191760 adds to the list of metal-rich multiple planet systems. The periods indicate the planets are located at the 10:1 mean motion resonance points. The outer planet exerts a large reflex velocity of  $322.17 \pm 18.98$  m/s on HD191760, whereas the inner planet’s amplitude is found to be  $24.22 \pm 2.86$  m/s. The best fit to the Doppler data suggest a low eccentricity of  $0.04 \pm 0.12$  for the inner planet and a somewhat larger eccentricity of  $0.49 \pm 0.07$  for the outer planet. Dynamical simulations show the system to be stable, at least for the next  $10^5$  years. However, the eccentricity of the inner planet is found to oscillate with a frequency of around 140 years which may be measurable with more epochs of high quality radial-velocity data. In addition we also refine the orbits found for HD48265*b*, HD143361*b* and HD154672*b*. These systems have been announced by the Magellan Planet Search.

## Key words:

stars: low-mass, brown dwarfs – planetary systems – techniques: radial velocities

## 1 INTRODUCTION

Since the first few extrasolar planets (hereafter exoplanets) were detected (Mayor & Queloz 1995; Marcy & Butler 1996a; Marcy & Butler 1996b) it became readily apparent that planets preferred metal-rich environments (Gonzalez 1997). This discovery has been placed in the framework of giant planet formation through core accretion of gas depleted materials left over from the formation of the parent star (e.g. Kornet et al. 2005; Alibert et al. 2005). This hypothesis has been extensively tested by different methods and analysis techniques, most recently by Fischer & Valenti (2005), and remains the most plausible scenario for the increased probability of planet detection around metal-rich stars. The competing theory is based on the concept that planets migrate through the proto-planetary disks from which they formed

(Lin & Papaloizou 1986; Trilling et al. 2002). It has been hypothesized that the stellar atmosphere is polluted after formation through infall of migrating planets onto the stellar surface. However, Pinsonneault et al. (2001) modelled the infall of material onto stellar atmospheres at the ZAMS and found that  $10M_{\oplus}$  worth of gas depleted material could raise the metallicities ( $[Fe/H]$ ) of G dwarfs to  $\sim 0.3$  dex, whereas the same material falling on an F dwarf would increase the metallicity to  $\sim 0.6$  dex. In their large sample ( $>1000$  stars) of consistent metallicities, Fischer & Valenti found no correlation between the depth of convective zones of exoplanet hosts and their metallicity, indicating that infall of planets or gas depleted material can not explain the over abundance of metal-rich atmospheres for exoplanet host stars.

Whatever the scenario that leads to exoplanet host stars being rich in metals, what is clear is that such stars have a higher probability of hosting exoplanets. Fischer & Valenti have determined that the fraction of planets increases with increasing metallicity proportional to the square of the number of iron atoms in the stellar photosphere. This correlation is being exploited by a number of planet search projects

\* Calan-Hertfordshire Extrasolar Planet Search

† Based on observations collected at the La Silla Paranal Observatory, ESO (Chile) with the HARPS spectrograph on the ESO 3.6m telescope, under the program IDs 079.C-0927(B), 079.C-0927(C), 081.C-0148(A) and 081.C-0148(B).

like the N2k, Keck, etc who bias their samples, or subsets thereof, towards the most metal-rich stars. We are exploiting this correlation also, by searching around the most metal-rich solar-type stars in the southern hemisphere as part of our CHEPS project. The CHEPS target list is compiled from the analysis of Jenkins et al. (2008) by utilising high S/N high resolution spectra, acquired using the FEROS spectrograph (Kaufer et al. 1999). The targets were selected to have  $[\text{Fe}/\text{H}] \geq 0.1$  dex and all have  $B-V$  colours in the range 0.5–0.9. Along with the metallicity bias we are also focusing on the most inactive stars. The Ca II HK line cores were used in Jenkins et al. to measure the  $\log R'_{\text{HK}}$  activity index (Noyes et al. 1984) which has been shown to be a useful proxy to the level of noise (aka *jitter*) in radial-velocity timeseries (Saar & Donahue 1997; Saar et al. 1998; Wright 2005). We therefore selected our primary sample to include all stars with  $\log R'_{\text{HK}} \leq -4.5$ , which allows for the lowest levels of radial-velocity jitter in our dataset.

## 2 OBSERVATIONS

We present data from four observing runs using the ESO-HARPS instrument (Mayor et al. 2003) on the 3.6m telescope in La Silla Chile. HARPS is a fiber-fed cross-dispersed echelle spectrograph. The instrument employs two  $1''$  on sky fibers, one on object and one on the Thorium-Argon (ThAr) calibration source, which feed the light to the spectrograph to be reimaged on two 2k4 CCD chips. 72 orders are spread over the two CCD's, 36 object and 36 calibration source, with an instrumental resolution ( $R$ ) of 115,000. 25 observations were made using our standard observational procedure, which aims to observe each star for a fixed integration time of 15 minutes in order to integrate over the strongest p-mode oscillations that all solar-like stars exhibit (O'Toole et al. 2008). Also to attempt to increase our efficiency to the detection of short period exoplanets, we heavily sample all potential planetary signals, including for HD191760.

The reduction and analysis of all stars are performed in near real time at the telescope, using the latest version of the HARPS-DRS (Pepe et al. 2004). The DRS (Data Reduction Software) performs all functions of the reduction and analysis, from bias removal, order localisation, flatfielding, cosmic ray removal, scattered light subtraction, extraction and blaze correction, to determination of the radial-velocities, barycentric Julian dates and internal uncertainties through cross-correlation with stellar templates and the reference ThAr calibration orders. Due to the high quality mechanical, thermal and pressure stabilisation of the HARPS instrument, the drift over a single night is found to be less than 1 m/s. Such a system provides internal uncertainties below 1 m/s, meaning our short term precision is dominated by stellar activity induced jitter (e.g. Saar et al. 1998).

## 3 HD191760 CHARACTERISTICS

Table 1 lists the stellar characteristics of the star HD191760. Houk (1978) lists the star's spectral type as G3IV/V, which is in agreement with the value adopted by Hipparcos (Perryman et al. 1997; Floor van Leeuwen 2008) and also with the derived distance from the Hipparcos main sequence

( $\Delta M_V$ ; Jenkins et al. 2008). All Hipparcos astrometry was obtained using the AstroGrid tool which lists the new catalogue values from van Leeuwen with increased astrometric precision. The kinematic catalogue of Nordström et al. (2004), later updated by Holmberg et al. (2007), includes observations of HD191760 through Strömgren filters and calibrations based on the infrared flux method (Alonso et al. 1996) to derive various stellar characteristics. They also used parallax measurements from Hipparcos, along with Padova evolutionary tracks (Girardi et al. 2000) to determine evolutionary parameters for their sample. We have also derived various parameters for a number of stars in preparation for our metallicity based planet search, both by high resolution FEROS spectra and precise photometry. We used the Hipparcos optical magnitudes, along with 2MASS photometry, to measure the effective temperatures of our stars by the infrared flux method (Blackwell et al. 1990). We used these temperatures to interpolate a grid of high resolution Kurucz model atmospheres (Kurucz 1993), built using WITA6 (Pavlenko 2000), to determine the stellar metallicity. Yonsei-Yale (Y2) isochrones (Demarque et al. 2004) were then interpolated using these temperatures, metallicities and an estimate for the alpha-enhancement parameter that was obtained by the locus of points in Edvardsson et al. (1993) and Pagel & Tautvaišienė (1995).

The properties of HD191760 derived by Holmberg et al. and this work agree within the formal uncertainties. Their metallicity value of  $0.12 \pm 0.10$  dex compares with our value of  $0.29 \pm 0.07$  dex. Fig. 1 shows the position of HD191760 on an HR-diagram, along with the Y2 isochrones in steps of  $0.1 M_{\odot}$  (solid curves) and higher resolution steps of  $0.01 M_{\odot}$  (dashed curves). The position of the star, given the bolometric luminosity of  $2.69 \pm 0.2 L_{\odot}$ , effective temperature of  $5821 \pm 82 \text{K}$  and  $[\text{Fe}/\text{H}]$  of  $0.29 \pm 0.07$ , is best explained by a star of mass  $1.28^{+0.02}_{-0.10} M_{\odot}$ , where the uncertainties are dominated by the uncertainty on the Hipparcos parallax. Our estimate for the age of the star is  $4.1^{+0.8}_{-2.8}$  Gyrs. The large lower error bar arises due to position of the star close to the main sequence turnoff. The surface gravity ( $\log g$ ) value of  $4.13^{+0.05}_{-0.04}$  dex is consistent with a star evolving onto the subgiant branch.

As part of the analysis we performed to select our target sample we also extracted chromospheric activity indices from measurements of the level of emission in the Ca II HK lines. The  $\log R'_{\text{HK}}$ -index has been shown to correlate well with the level of noise (aka jitter) in precise radial-velocity datasets (e.g. Santos et al. 2000; Wright 2005). Fig. 2 shows the Ca II H line core of HD191760 (top) along with the other three planet-host stars we present data for in §5. Our low derived value of  $\log R'_{\text{HK}} = -5.17$  can be visually seen from the deep central line core of HD191760. We use an updated version of the Wright relation (private communication) to estimate a value of 2.40 m/s for the activity induced jitter of HD191760.

## 4 ORBITAL SOLUTION FOR HD191760

The 25 Doppler velocities for HD191760 were measured in four observing runs spanning five nights in duration each and are listed in Table 2. In Fig. 3 (top panel) we show the best fit double planet Keplerian to the observed radial

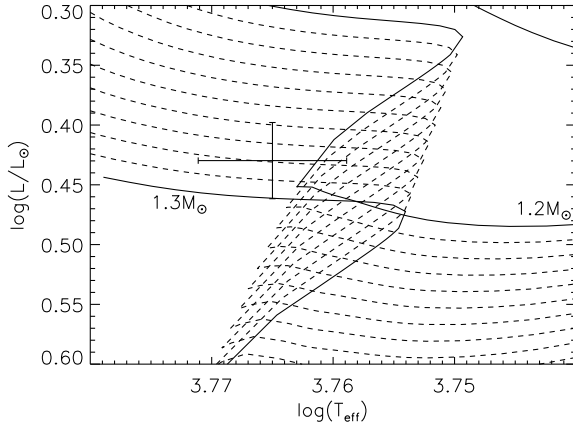


**Figure 1.** Evolutionary Y2 mass tracks are shown in steps of  $0.1M_{\odot}$  (solid curves) and finer steps of  $0.01M_{\odot}$  (dashed curves) for effective temperatures and bolometric luminosities. HD191760 is represented by the error bars and its position is consistent with a mass of  $1.28^{+0.02}_{-0.10}M_{\odot}$  and an age of  $4.21^{+0.5}_{-2.8}$  Gyrs. The masses of the solid curves are shown for reference.

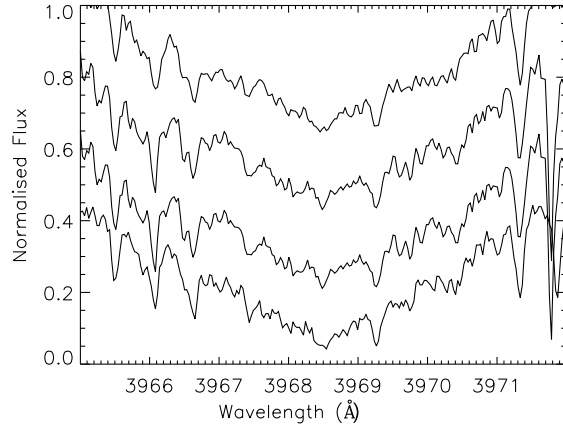


**Figure 2.** The calcium II H line cores for the four stars discussed in this work. From top to bottom we show HD191760, HD48265, HD143361 and HD154672 respectively. All four objects exhibit no re-emission of flux in the line core, highlighting the inactive nature of these stars.

**Table 1.** Stellar parameters for HD191760.

Parameter	HD191760
Spectral Type	G3IV/V
$\log R'_{\text{HK}}$	-5.17
Hipparcos $N_{\text{obs}}$	99
Hipparcos $\sigma$	0.011
$\Delta M_V$	1.107
$L_{\star}/L_{\odot}$	$2.69 \pm 0.20$
$M_{\star}/M_{\odot}$ - H07	$1.14^{+0.08}_{-0.05}$
$M_{\star}/M_{\odot}$ - Here	$1.28^{+0.02}_{-0.10}$
$R_{\star}/R_{\odot}$	$1.62 \pm 0.07$
$T_{\text{eff}}$ (K) - H07	$5794 \pm 76$
$T_{\text{eff}}$ (K) - J08	$5821 \pm 82$
[Fe/H] - H07	$0.12 \pm 0.10$
[Fe/H] - J08	$0.29 \pm 0.07$
$\log(g)$	$4.13^{+0.05}_{-0.04}$
U,V,W - H07 (km/s)	-29,-21,15
$v \sin i_{R'_{\text{HK}}}$ (km/s)	3.47
$v \sin i_{\text{H07}}$ (km/s)	2
$v \sin i_{\text{CCF}}$ (km/s)	$2.33 \pm 0.05$
$P_{\text{rot}, R'_{\text{HK}}}$ (days)	25.2
$P_{\text{rot}, \text{CCF}}$ (days)	38
Age $_{R'_{\text{HK}}}$ (Gyrs)	9.9
Age (Gyrs) - H07	$5.6^{+0.9}_{-1.9}$
Age (Gyrs) - Here	$4.1^{+0.8}_{-2.8}$
Jitter - $\log R'_{\text{HK}}$ (m/s)	2.40

H07 relates to Holmberg et al. (2007), J08 is the reference for Jenkins et al. (2008) and HERE labels values derived in this work.

velocity timeseries derived from Systemic (Maschiarì 2008). Our observations span five orbital periods of HD191760c and also sample HD191760b due to our method of multiple observations through each observing run. This technique allows us to extract the double planet fit much faster than typical radial-velocity sampling strategies. To quantify the double planet solution an F-test revealed a lower than 1% probability that a single planet solution and double planet solution are statistically similar. The reduced  $\chi^2$  is 0.87, with a resid-

ual rms of only 1.75 m/s, highlighting the robustness of the double Keplerian to describe the data. The uncertainties are all within the plotting symbols at this scale. These uncertainties are a combination of both internal precision and expected stellar jitter. Since the  $\log R'_{\text{HK}}$  is extremely low (-5.17) and the star is evolving away from the main sequence we expect the jitter to be fairly low. The updated Wright jitter model, explained above, for stars with  $\Delta M_V \geq 1$  gives a median of 2.40 m/s. This jitter is added in quadrature with the internal errors provided by the HARPS-DRS.

Fig. 3 (top-middle) shows the residuals to the double planet solution and highlights the robustness of the fit given the small number of epochs. The outer planet has a period of  $86.83 \pm 0.50$  days, an eccentricity of  $0.50 \pm 0.07$ , semimajor axis of 0.42 AU and a semi-amplitude ( $K$ ) of  $322.17 \pm 17.39$  m/s. This gives rise to a planet with a minimum mass ( $m \sin i$ ) of  $7.20 \pm 0.44 M_J$ . However, the relatively small number of observing epochs means that there could be a variety of more complex multiple planet solutions. Given the relatively short period of the signature, this can be robustly tested with more data.

From the last observing run it was clear that a one planet Keplerian could not describe the observations, which would have been the case if we had simply observed this system one velocity point per observing run. There appears a clear coherence in the velocities after the large outer planet is removed, highlighted by the lower two panels. Fig. 3 (middle-bottom) shows the fit to the outer planet alone and there is a clear variation in the velocities that can not be explained by a single planetary fit. The bottom panel shows the phased residuals to this fit. We find the best fit to this signal is explained by a short period, sub Jupiter-mass planet. The period of the signal is found to be  $8.64 \pm 0.02$  days, with a semi-amplitude of  $24.22 \pm 4.14$  m/s, a low eccentricity of  $0.04 \pm 0.12$  and semimajor axis of 0.09 AU. The minimum mass of this planet is found to be  $0.29 \pm 0.05 M_J$ . All orbital parameters for these objects are shown in columns 1 and 2 of Table. 4.

Finally, Fig. 4 shows the bisector span (O-C) versus the radial-velocity data. Such a diagnostic tool can be used to disentangle the effects of line variations in the stellar spec-

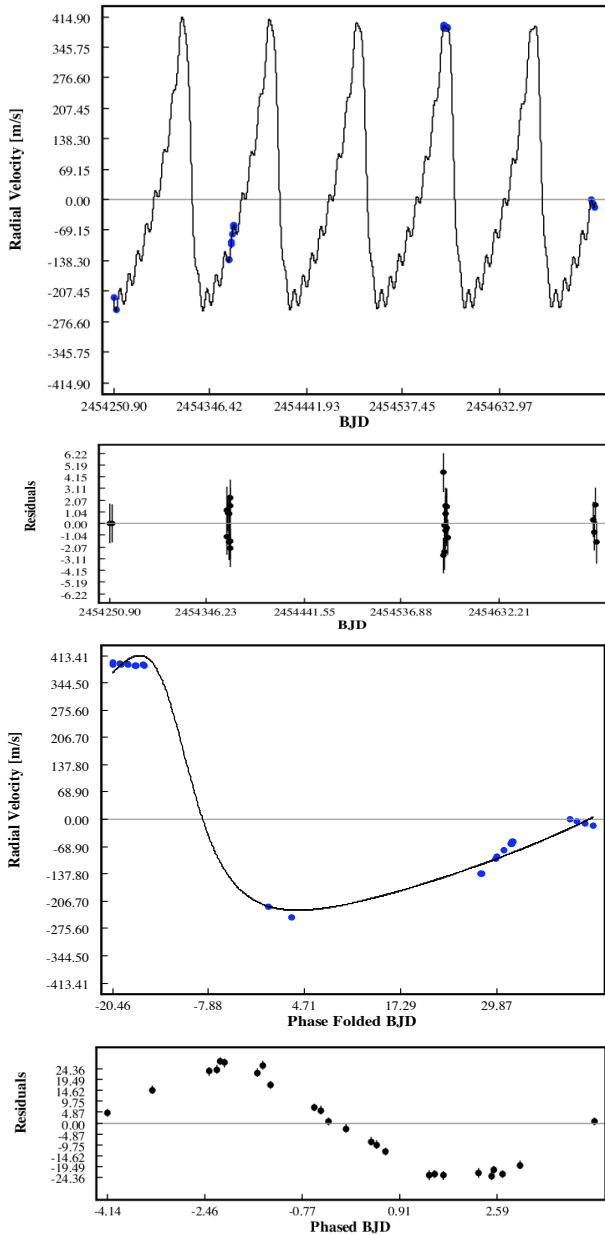


**Figure 3.** The top panel shows the best fit double Keplerian solution to the Doppler points for HD191760. The data come from four observing runs spread over five orbits of the outer planet. The top-middle plot shows the residuals to the this double planet fit and highlights the fit is robust within the adopted uncertainties. The lower-middle plot shows the fit to the data with the inner planetary signal removed and visually highlights the variation of the data without adopting a secondary short period planet. The bottom panel shows the residuals to this single planet fit phased to the determined period of the inner planet’s signature. It is clear that this planet’s orbital period has been well sampled. The uncertainties represent the HARPS measurement precision added in quadrature with the estimated activity induced jitter.

trum and the appearance of any radial-velocity variations (see Queloz et al. 2001). It is clear there is no significant correlation, highlighted by the lack of any significant slope in the best fit trend line plotted through the data, which adds weight to the origin of the signature being by orbiting planets rather than line modulations from sources such

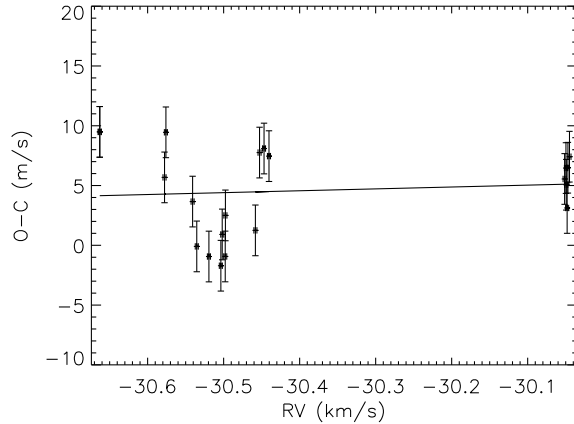


**Figure 4.** A plot of the bisector span against the measured radial-velocities, along with the best straight line fit to the data. There is clearly no significant correlation between these velocities and the CCF bisector.

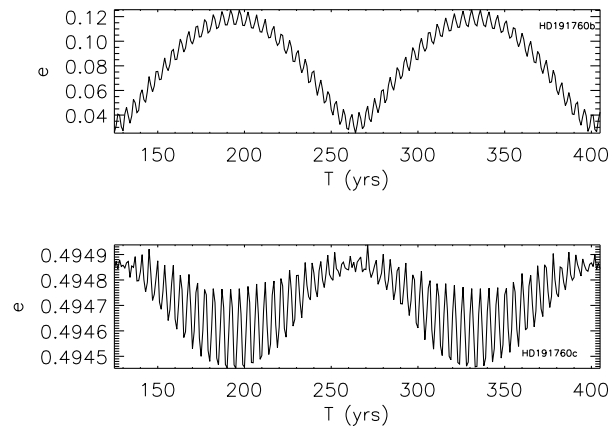


**Figure 5.** The eccentricity evolution of the two planets over a baseline of 280 years. The upper panel shows the eccentricity evolution of the inner planet (HD191760*b*), whereas the lower panel shows the same for the outer planet (HD191760*c*). The inner planet’s eccentricity undergoes oscillations of  $\sim \pm 0.05$  over the 140 year period, whereas the outer more massive planet undergoes little eccentricity change over the same timescale.

as star spots. Indeed, such a result was expected given the extremely inactive nature of the host star.

The uncertainties on the above orbital parameters should accurately represent the spread in probable values since we utilised a bootstrap method to constrain them. Although there is a reasonably small uncertainty on the eccentricity of HD191760*c*, it is still plausibly a circular orbit since studies indicate a bias against zero eccentricity for fairly low numbers of data points, admittedly with different sampling strategies to ours (Shen & Turner 2008; O’Toole et al. 2008).

The configuration of the system is such that the planets are located at the 10:1 mean motion resonance points. Also since the inner planet has an orbit consistent with zero and the outer massive planet appears to have a fairly large eccentricity we ran a dynamical simulation to test the stability of the system. The Runge-Kutta simulation algorithm is part of the Systemic code and was run on all parameters for the double planet solution across a time baseline of  $10^5$

years, in time steps of 1 day. The simulation revealed that the system is stable, for at least the next  $10^5$  years. Fig. 5 shows the eccentricity evolution of the two bodies, with the upper panel showing the inner planet (HD191760*b*) and the lower panel the outer planet (HD191760*c*). The eccentricities for the inner planet show significant oscillation on short period timescales ( $\sim 140$  years). This oscillation is driven by the tidal interactions between the inner planet and the massive outer planet as it moves around its fairly eccentric, 87 day orbit. Although this oscillation is within the current bootstrap uncertainties, with more high quality data it will be significantly reduced, which makes the system ideal for long term study since with high precision radial-velocities, this short term eccentricity evolution may be observable and allow short term model testing. The outer planet undergoes no significant eccentricity evolution due to its large mass and its orbital distance from the star.

#### 4.1 Probability of Transit

Since HD191760 is found to be both metal-rich and on the subgiant branch, the radius is larger than that found for typical main sequence G stars ( $R_*/R_\odot = 1.62 \pm 0.07$ ). If we assume both planets have radii equal to that of Jupiter, then the probability of transit is found to be 1.2% for the outer planet and 7.8% for the inner hot Jupiter type planet (Seagroves et al. 2003). Such probabilities make this an inviting target for further photometric follow-up to search for any transit signature(s) and we plan to follow up the star with high precision photometry to search for any transit signature. Indeed, a probability of 7.8% is approaching the probability of transit found for a number of the current crop of transiting exoplanets. Any transit discovery would add to the small number of bright transit planets where ground and space-based follow-up analysis can be performed to probe the planetary atmospheric characteristics.

The rotation velocity of the star is found to be  $2.33 \pm 0.05$  km/s, using a similar method to that explained in Santos et al. (2002) (the uncertainty is derived from the standard deviation of the 25 cross correlation full widths at half maximum), which for the determined radius we find gives an upper limit to the rotation period of 38 days. The estimated rotation period from the  $\log R'_{\text{HK}}$ -rotation period correlation (Noyes et al. 1984) is 25.2 days, which is inclination independent and should represent the equatorial rotation period, assuming that the orbital and rotation axes are aligned in the same plane. Assuming the rotation period from the activity relation holds then we estimate the system has a  $\sin i = 0.67$ , relating to an inclination ( $i$ ) of  $\sim 42^\circ$ , which is highly inclined, and would not be favourable for transit studies. However, the  $\log R'_{\text{HK}}$  activity index was formulated for stars on the main sequence and may be gravity dependent so would not be fully applicable to this star. Also the use of this index should be made only after a number of stellar cycles have been observed, which allows one a robust estimate of the mean  $\log R'_{\text{HK}}$ . We have applied the value quoted in Jenkins et al. (2008) (one measurement), not the mean, so we do not know the spread, which can vary at the  $\pm 0.1$  dex level (see Jenkins et al. 2006), and can not apply this to the uncertainty on the relationship itself, which Noyes et al. quote as 0.08 dex for the convective overturn time.

**Table 2.** Radial-velocities for HD191760

BJD (-2454000)	RV (m/s)	Uncertainty (m/s)
250.90047	-222.05	2.56
253.89490	-248.21	2.50
365.50781	-137.03	2.76
365.73781	-136.85	2.48
367.49679	-99.92	2.43
367.72155	-94.44	2.51
368.49981	-78.46	2.46
369.49468	-62.73	2.52
369.62706	-60.95	2.45
369.68010	-56.75	2.45
369.74838	-57.00	2.48
577.77658	395.93	2.54
577.90446	389.52	2.43
578.77151	393.87	2.46
578.90713	391.26	2.45
579.74685	392.82	2.46
579.90348	391.67	2.44
580.74769	388.80	2.47
580.89930	388.97	2.45
581.76210	391.09	2.43
581.91331	388.36	2.43
724.55839	0.58	2.42
725.53823	-5.94	2.44
726.53101	-11.83	2.44
727.53134	-17.30	2.64

## 5 REFINED ORBITS FOR THE PLANETS AROUND HD48265, HD143361 AND HD154672

Due to some overlap in our target sample with that of the Magellan Planet Search, we can update a few of the recent planet discoveries announced by this program with additional velocities we have found at HARPS. Table. 3 shows our absolute Doppler velocities for the three planet host stars HD48265, HD143361 and HD154672. For all of these stars we have acquired observations in three observing runs with overall baselines around one year in duration. Fig. 6 show the best fits to all three stars, with the Magellan velocities in blue and our HARPS values in green.

We show the updated orbital solutions in columns 3, 4 and 5 of Table. 4 and in general they agree well with the published results in both Minniti et al. (2008) (HD48265 and HD143361) and López-Morales et al. (2008) (HD154672). Lopez-Morales et al. used 16 velocity points in their orbital solution for HD154672 over a number of orbital periods of the planet. We find a very similar solution with a slightly reduced rms of 3.37 m/s. Note that we used the stellar masses quoted by this group for a direct comparison of the results found. For HD48365 we also find agreement in derived properties, though we find an improvement (factor of 2) in formal parameters when we remove two of their velocities with the largest uncertainties (this is the solution we quote in the table). The rms for this solution is found to be 3.37 m/s, whereas the rms for the best fit that includes the two data points with the largest uncertainties is 6.78 m/s. Finally, for HD143361*b* we find good agreement with the published results, again with a slightly reduced orbital period of 1056 days and eccentricity of 0.15. This relates to an

**Table 3.** Radial-velocities for HD48265, HD143361 and HD154672

BJD (-2454000)	RV (m/s)	Uncertainty (m/s)
HD48265		
365.824572	23394.21	3.47
366.874164	23399.40	3.50
367.852214	23395.69	3.45
580.522907	23449.18	3.45
581.553905	23450.06	3.45
724.833698	23413.42	3.45
725.817765	23414.08	3.44
726.779101	23411.87	3.47
HD143361		
250.745318	-437.90	2.39
253.769447	-436.44	3.23
367.556628	-474.74	2.22
368.537299	-474.20	2.24
578.788567	-534.13	2.18
581.807762	-531.75	2.19
HD154672		
248.713853	-3796.59	4.79
250.731312	-3794.42	2.25
367.595129	-3653.29	2.15
368.618599	-3651.00	2.22
578.811238	-3797.81	2.14
581.870548	-3808.85	2.13

M<sub>sin</sub>i of 3.12 M<sub>J</sub>, in good agreement with the 3 M<sub>J</sub> found by Minniti et al. and with a lower rms of 3.37 m/s. None of these three systems exhibit significant trends in the residuals and hence present no evidence as yet for additional planets in the system. Note the uncertainties shown in Table. 3 are again derived using the updated Wright relation and the low level of each is highlighted in Fig. 2 where no Ca II H line core emission is seen in any of these three stars (HD48265: top-middle, HD143361: lower-middle and HD154672: bottom).

## 6 SUMMARY

We announce the first exoplanet detections from the CHEPS on the ESO-HARPS instrument. The highlight is the discovery of two planets orbiting the metal-rich G3IV-V star HD191760. HD191760*b* and *c* are found to have masses of  $0.29 \pm 0.05$  and  $7.20 \pm 0.44$  M<sub>J</sub> and orbital periods of  $8.64 \pm 0.02$  and  $86.83 \pm 0.50$  days respectively and add to the list of metal-rich multiple planet systems. The planets are found to be located at the 10:1 mean motion resonance points and dynamical simulations suggest they are held in a stable configuration for at least the next  $10^5$  years. The eccentricity of the inner planet appears to undergo short term evolution and the scale of these oscillations may be observable with more data over the long term. The discovery of this double system with only 25 Doppler points in four observing runs over a baseline of less than 500 days, highlights the efficient nature of our observational strategy, even when they are found to be of fairly long period. Had we sampled in single velocity points per observing run, this system would have taken years to constrain.

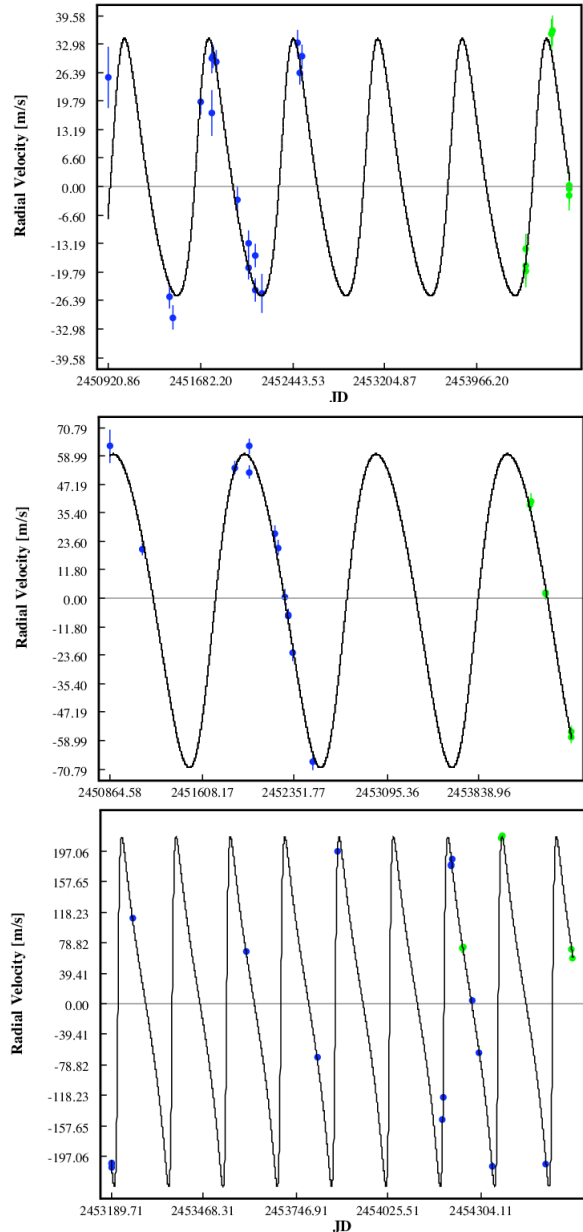


**Figure 6.** The radial-velocity Keplerian fits to the stars HD48265 (top), HD143361 (middle) and HD154672 (bottom). Plotted in blue are the literature values from the Magellan program and in green are the new data points from here.

Finally, we also confirm the exoplanet detections of HD48265*b*, HD143361*b* and HD154672*b* from the Magellan program. We show updated orbits by adding eight velocities for HD48265 and six velocities each for HD143361 and HD154672. All orbital parameters are in good agreement with the published results by this group, with slightly reduced rms. Such confirmations highlight our technique is robust and allows us to continue with confidence using this strategy in the future.

### Acknowledgements

J.S.J acknowledges partial support from Centro de Astrofísica FONDAF 15010003, along with partial support from GEMINI-CONICYT FUND and partial support from Comité Mixto ESO-GOBIERNO DE CHILE. We also ac-

**Table 4.** Orbital parameters for HD191760b, HD191760c, HD48265b, HD143361b and HD154672b.

Parameter	HD191760b	HD191760c	HD48265b	HD143361b	HD154672b
Orbital period $P$ (days)	8.64±0.02	86.83±0.50	696±8	1057±20	163.9±0.1
Velocity amplitude $K$ (m/s)	24.22±4.14	322.17±17.39	29.7±7.0	65.1±26.3	226.52±9.22
Eccentricity $e$	0.04±0.12	0.50±0.07	0.25±0.16	0.15±0.17	0.61±0.02
$\omega$ (°)	29±112	55±7	307±32	237±55	266±2
$M\sin i$ ( $M_J$ )	0.29±0.05	7.20±0.44	1.20±0.72	3.12±1.44	5.02±0.17
Semimajor axis $a$ (AU)	0.09	0.42	1.50	2.00	0.60
rms (m/s)	1.75	–	3.47	3.37	3.37
$\chi^2_\nu$	0.87	–	2.11	2.42	2.14
$N_{\text{Obs}}$	25	–	25*	18	22
$P_{\text{transit}}$	0.078	0.012	–	–	–

The rms,  $\chi^2_\nu$  and  $N_{\text{Obs}}$  for both HD191760b and c are for the two planet fit therefore they are only shown once, in the HD191760b column. \* This represents the total number of data points, even though the fit parameters remove the two with the largest uncertainties. No transit probabilities are shown for the planets discovered by the Magellan program since they have sufficiently long periods to render the probabilities extremely low.

knowledge the Simbad and VizieR astronomical databases. This research has made use of data obtained using the UK's AstroGrid Virtual Observatory Project, which is funded by the Science & Technology Facilities Council and through the EU's Framework 6 programme.

## REFERENCES

- Alibert Y., Mordasini C., Benz W., Winisdoerffer C., 2005, *A&A*, 434, 343
- Alonso A., Arribas S., Martinez-Roger C., 1996, *A&A*, 313, 873
- Blackwell D. E., Petford A. D., Arribas S., Haddock D. J., Selby M. J., 1990, *A&A*, 232, 396
- Demarque P., Woo J.-H., Kim Y.-C., Yi S. K., 2004, *ApJS*, 155, 667
- Edvardsson B., Andersen J., Gustafsson B., Lambert D. L., Nissen P. E., Tomkin J., 1993, *A&A*, 275, 101
- Fischer D. A., Valenti J., 2005, *ApJ*, 622, 1102
- Floor van Leeuwen L., 2008, *VizieR Online Data Catalog*, 1311, 0
- Girardi L., Bressan A., Bertelli G., Chiosi C., 2000, *A&AS*, 141, 371
- Gonzalez G., 1997, *MNRAS*, 285, 403
- Holmberg J., Nordström B., Andersen J., 2007, *A&A*, 475, 519
- Houk N., 1978, Michigan catalogue of two-dimensional spectral types for the HD stars. Ann Arbor : Dept. of Astronomy, University of Michigan : distributed by University Microfilms International, 1978-
- Jenkins J. S., Jones H. R. A., Pavlenko Y., Pinfield D. J., Barnes J. R., Lyubchik Y., 2008, *ArXiv e-prints*, 804
- Jenkins J. S., Jones H. R. A., Tinney C. G., Butler R. P., McCarthy C., Marcy G. W., Pinfield D. J., Carter B. D., Penny A. J., 2006, *MNRAS*, 372, 163
- Kaufer A., Stahl O., Tubbesing S., Norregaard P., Avila G., Francois P., Pasquini L., Pizzella A., 1999, *The Messenger*, 95, 8
- Kornet K., Bodenheimer P., Różyczka M., Stepinski T. F., 2005, *A&A*, 430, 1133
- Kurucz R., 1993, *ATLAS9 Stellar Atmosphere Programs and 2 km/s grid*. Kurucz CD-ROM No. 13. Cambridge, Mass.: Smithsonian Astrophysical Observatory, 1993., 13
- Lin D. N. C., Papaloizou J., 1986, *ApJ*, 309, 846
- López-Morales M., Butler R. P., Fischer D. A., Minniti D., Shectman S. A., Takeda G., Adams F. C., Wright J. T., Arriagada P., 2008, *AJ*, 136, 1901
- Marcy G. W., Butler R. P., 1996a, *ApJL*, 464, L147+
- Marcy G. W., Butler R. P., 1996b, in *Proc. SPIE Vol. 2704*, p. 46-49, *The Search for Extraterrestrial Intelligence (SETI) in the Optical Spectrum II*, Stuart A. Kingsley; Guillermo A. Lemarchand; Eds. First three planets. pp 46–49
- Maschiarri S., 2008, in prep
- Mayor M., Pepe F., Queloz D. e. a., 2003, *The Messenger*, 114, 20
- Mayor M., Queloz D., 1995, *Nature*, 378, 355
- Minniti D., Butler R. P., Lopez-Morales M., Shectman S. A., Adams F. C., Arriagada P., Boss A. P., Chambers J. E., 2008, *ArXiv e-prints*
- Nordström B., Mayor M., Andersen J., Holmberg J., Pont F., Jørgensen B. R., Olsen E. H., Udry S., Mowlavi N., 2004, *A&A*, 418, 989
- Noyes R. W., Hartmann L. W., Baliunas S. L., Duncan D. K., Vaughan A. H., 1984, *ApJ*, 279, 763
- O'Toole S. J., Tinney C. G., Jones H. R. A., 2008, *MNRAS*, 386, 516
- O'Toole S. J., Tinney C. G., Jones H. R. A., Butler R. P., Marcy G. W., Carter B., Bailey J., 2008, *ArXiv e-prints*
- Pagel B. E. J., Tautvaisiene G., 1995, *MNRAS*, 276, 505
- Pavlenko Y. V., 2000, *Astronomy Reports*, 44, 219
- Pepe F., Mayor M., Queloz D., Benz W., Bonfils X., Bouchy F., Curto G. L., Lovis C., Mégevand D., Moutou C., Naef D., Rupprecht G., Santos N. C., Sivan J.-P., Sosnowska D., Udry S., 2004, *A&A*, 423, 385
- Perryman M. A. C., Lindegren L., Kovalevsky e. a., 1997, *A&A*, 323, L49
- Pinsonneault M. H., DePoy D. L., Coffee M., 2001, *ApJL*, 556, L59
- Queloz D., Henry G. W., Sivan J. P., Baliunas S. L., Beuzit J. L., Donahue R. A., Mayor M., Naef D., Perrier C., Udry S., 2001, *A&A*, 379, 279
- Saar S. H., Butler R. P., Marcy G. W., 1998, *ApJL*, 498,

L153

- Saar S. H., Donahue R. A., 1997, *ApJ*, 485, 319  
Santos N. C., Mayor M., Naef D., Pepe F., Queloz D., Udry S., Blecha A., 2000, *A&A*, 361, 265  
Santos N. C., Mayor M., Naef D., Pepe F., Queloz D., Udry S., Burnet M., Clausen J. V., Helt B. E., Olsen E. H., Pritchard J. D., 2002, *A&A*, 392, 215  
Seagroves S., Harker J., Laughlin G., Lacy J., Castellano T., 2003, *PASP*, 115, 1355  
Shen Y., Turner E. L., 2008, *ApJ*, 685, 553  
Trilling D. E., Lunine J. I., Benz W., 2002, *A&A*, 394, 241  
Wright J. T., 2005, *PASP*, 117, 657